

***In situ* XAFS Analysis for Thermochemical Conversion Process of CoCl<sub>2</sub> on SiO<sub>2</sub>****Misato Katayama, Asaka Azuma, Sojiro Shibata, and Yasuhiro Inada***Department of Applied Chemistry, Graduate School of Life Sciences, Ritsumeikan University, 1-1-1 Noji-Higashi, Kusatsu 525-8577, Japan*

The thermochemical conversion processes, in which CoCl<sub>2</sub> supported on silica is reduced to Co(0) by gaseous H<sub>2</sub> and Co(0) is chlorinated to CoCl<sub>2</sub> by gaseous Cl<sub>2</sub>, were analyzed by means of *in situ* XAFS method. It was found that both the reduction and the chlorination process between CoCl<sub>2</sub> and Co(0) proceed in a single step. The temperature of reduction of CoCl<sub>2</sub> is lower than that of CoO, and the temperature of chlorination of Co(0) is higher than that of oxidation. The results indicate that there are differences in reactivity in conversion depending on the type of anion.

**1. Introduction**

In the case of XAFS measurements using X-rays in a hard X-ray region, the high permeability of the X-rays allows for a relatively free layout around the sample. The advantage of *in situ* measurement is not only to obtain information on the state under actual operating conditions, but also to extract minute changes in the sample of interest without being affected by errors due to differences in sample preparation lots, etc., by continuously measuring the same measurement points on the same sample. We have studied that the change in the chemical state of transition metal particles in the solid phase using *in situ* XAFS analysis and revealed the dissociation and insertion mechanism of oxide ions during the thermochemical conversion process between metal oxide and metal [1-4].

In recent years, attention has been focused on systems that use solid-state redox reactions of metal particles as electrode reactions in storage batteries. Metal oxides and metal halides are expected to be the candidates because they have the potential to achieve high capacity [5-7]. Metal chlorides are promising as next-generation materials from the viewpoints of safety and cost [8-10]. The process of dissociation and insertion of anions in the solid phase involves the exchange of electrons, thus understanding this mechanism is important in the development of high-performance electrode materials. Because the electrodes contain conductive additives and binders in addition to the active material, observing the reaction only in the process, in which active material particles take in and out the anions, is a good indicator for understanding reactions in the electrode. In this study, we used *in situ* XAFS method to analyze the process in which Co(II) chloride particles release chloride ions to become Co(0) particles, and Co(0) particles incorporate chloride ions to become Co(II) chloride particles. The reactions proceeded by using inert and stable silica as a supporting material and increasing the temperature under a flow of gaseous reactants. Because the diffusion of reactant gas does not affect the conversion of the Co species, it is expected that

the characteristics of the conversion of the CoCl<sub>2</sub>/Co pair can be revealed from the obtained reaction temperature. By comparing the conversion temperature of the CoCl<sub>2</sub>/Co pair with that of the CoO/Co pair, the characteristics of their conversion processes will be discussed.

**2. Experimental***Preparation*

The powder sample of CoCl<sub>2</sub> supported on SiO<sub>2</sub> (JRC-SIO-10) was prepared by an incipient wetness impregnation method for the *in situ* XAFS measurements of the temperature-programmed reduction (TPR) and the temperature-programmed chlorination (TPC) processes. An aqueous solution of CoCl<sub>2</sub>·6H<sub>2</sub>O (Fujifilm Wako Pure Chemical) was added to SiO<sub>2</sub> and dried at 60 °C for 6 h under air. The loading of CoCl<sub>2</sub> was adjusted to be 20 wt%.

*Characterization*

The X-ray diffraction (XRD) measurement was performed using the Ultima IV diffractometer (Rigaku) using Cu K<sub>α</sub> radiation. The diffraction intensities were recorded in the 2θ values between 10° and 80°. The loading of supported CoCl<sub>2</sub> was determined by the X-ray fluorescence analysis (XRF) using the Supermini fluorescent X-ray spectrometer (Rigaku). A calibration curve was obtained using a sample in which a known amount of CoCl<sub>2</sub> hydrate was physically mixed with SiO<sub>2</sub>. The mass change of the prepared sample at the elevated temperature was measured using a thermogravimetric and differential thermal analysis (TG-DTA) instrument DTG-60/60H (Shimadzu).

*In situ XAFS measurement*

The *in situ* XAFS measurements were carried out in the transmission mode using a Si(220) and Si(111) double-crystal monochromator at BL-3 of the SR Center (Ritsumeikan Univ.) and at BL-9C of the Photon Factory (KEK). The higher-order reflections of the monochromator were removed by detuning the parallelism for the measurements at the Photon Factory. The TPR process was performed at BL-9C

(Photon Factory) under an H<sub>2</sub> gas diluted by He (10 vol%) with a total flow rate of 100 cm<sup>3</sup>/min. The TPC process was performed at BL-3 (SR Center) under a Cl<sub>2</sub> gas diluted by N<sub>2</sub> (1 vol%) with a total flow rate of 100 cm<sup>3</sup>/min. The amount of sample required for the XAFS measurements at the Co K edge was estimated based on the absorption coefficient and filled into a quartz glass ring with an inner diameter of 7 mm. Then, the sample ring was placed in a flow-type *in situ* XAFS cell. The harmful gases such as Cl<sub>2</sub> and HCl were removed by installing a gas trap with 2 M NaOH solution downstream of the glass cell.

### 3. Results and Discussion

#### 3.1. Initial state

Figure 1(A) shows a XANES spectrum of the prepared sample compared with a standard sample of

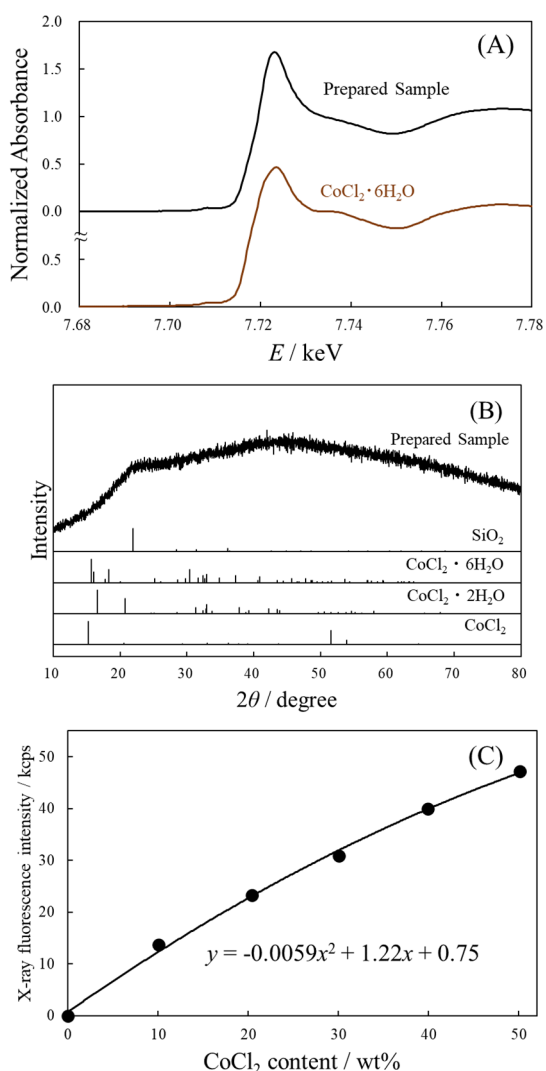
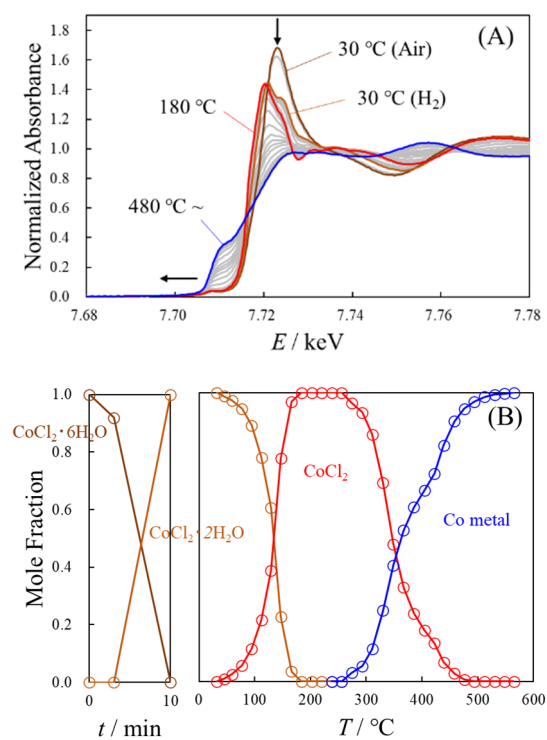


**Fig. 1.** The characterization of the prepared sample by the XANES spectra (A) and the XRD pattern (B). The loading of CoCl<sub>2</sub> was determined by the XRF measurement based on the calibration curve depicted in (C).

cobalt(II) chloride hexahydrate. Two samples showed the consistent absorption edge and white line. It is thus identified that the Co(H<sub>2</sub>O)<sub>6</sub>Cl<sub>2</sub> is supported on silica in the prepared sample. The XRD data of the prepared sample is given in Fig. 1(B). No diffraction peaks derived from the Co species were observed, suggesting that Co(H<sub>2</sub>O)<sub>6</sub>Cl<sub>2</sub> exists in an amorphous state. The loading of CoCl<sub>2</sub> of the prepared samples was determined by the XRF measurement. The calibration curve obtained by plotting the X-ray fluorescence intensity against the CoCl<sub>2</sub> content of the standard sample is shown in Fig. 1(C). The calibration curve was expressed as a quadratic function of  $y = ax^2 + bx + c$  ( $y$ : the X-ray fluorescence intensity in kcps,  $x$ : the content of CoCl<sub>2</sub>), where  $a = -0.0059$ ,  $b = 1.22$ , and  $c = 0.75$ . The X-ray fluorescence intensity of the prepared sample (20.94 kcps) derived the actual loading of CoCl<sub>2</sub> to be 18.1 wt%.

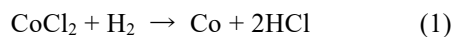
#### 3.2. Reduction Process

Figure 2(A) shows the XANES spectral change during the TPR process of the CoCl<sub>2</sub> species on silica by gaseous H<sub>2</sub>. The initial spectrum was consistent with that of Co(H<sub>2</sub>O)<sub>6</sub>Cl<sub>2</sub>, which was changed to CoCl<sub>2</sub>·2H<sub>2</sub>O at room temperature under the gas flow of dry H<sub>2</sub> and He. The XANES spectrum further changed to 180 °C, but the absorption edge energy was almost maintained at that time. Considering the



**Fig. 2.** The change of the XANES spectra (A) and the mole fraction of the Co species (B) during the TPR process of CoCl<sub>2</sub> on silica.

results of TG-DTA analysis described below, it was found that anhydrous  $\text{CoCl}_2$  is generated at 180 °C. At higher temperatures, the white line intensity at 7.72 keV decreased and the absorption edge shifted to the lower side. The final spectrum almost matched that of Co metal, indicating that the two-electron reduction of anhydrous  $\text{CoCl}_2$  to Co(0) represented by eq. (1) proceeded.



The mole fraction of the Co species estimated by a linear combination fitting (LCF) analysis of the XANES spectrum is plotted as a function of temperature in Fig. 2(B). The change from the initial state to the dihydrate was completed by keeping at room temperature for 10 min, thus the spectra before and after that were used as the standard. In addition, the spectra at 180 °C as anhydrous  $\text{CoCl}_2$  and the final state as Co(0) were used. The desorption of two  $\text{H}_2\text{O}$  molecules in the dihydrate proceeded at 120 °C, and anhydrous  $\text{CoCl}_2$  exists in the range of 180 to 250 °C. Reduction of  $\text{CoCl}_2$  to Co(0) progressed at temperatures above 300 °C, and the reduction was completed at temperatures above 500 °C.

The TG-DTA curves of the prepared sample are shown in Fig. 3(A). The weight is constant above 160 °C and it is reasonably assumed that anhydrous  $\text{CoCl}_2$  is generated in that temperature range. Assuming that the final weight of 17.3 mg is silica

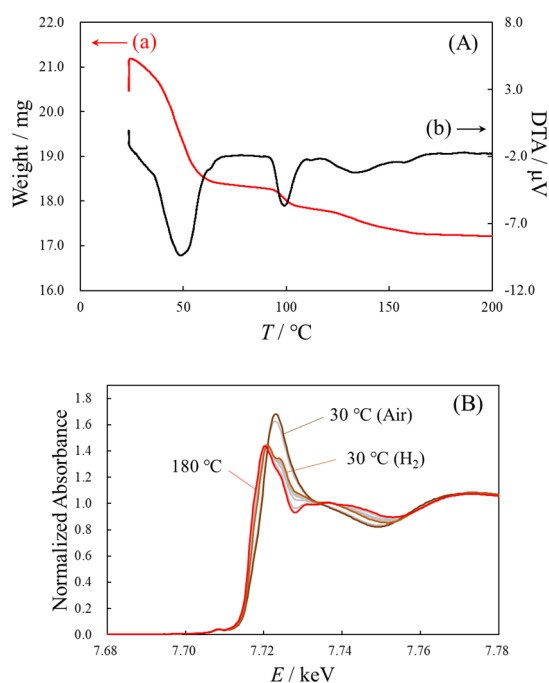
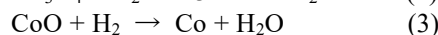


**Fig. 3.** TG-DTA curves (A) of the prepared sample in the temperature range up to 200 °C. The XANES spectral change at the same temperature range is shown in (B).

containing 18.1 wt% anhydrous  $\text{CoCl}_2$ , it would be calculated to be 20.2 mg if  $\text{Co}(\text{H}_2\text{O})_6\text{Cl}_2$  exists at the beginning. Because the initial weight was even higher, it was considered that there was also water adsorbed on the silica in addition to the six hydrated waters. The weight was constant at 18.3 mg in the temperature range from 60 °C to 90 °C. A weight loss of 1.0 mg from 90 °C to above 160 °C corresponds to the weight of 2 equivalents of water relative to Co. This means that  $\text{CoCl}_2 \cdot 2\text{H}_2\text{O}$  is generated between 60 °C and 90 °C, and changes to anhydrous  $\text{CoCl}_2$  above 160 °C.

The XANES spectral change in the same temperature range during the TPR process is shown again in Fig. 3(B). The initial spectrum with a sharp white line corresponds to the hexahydrate, and the dihydrate forms when kept in a dry environment at room temperature. This corresponds to the endothermic weight loss accompanied at around 50 °C observed in TG-DTA. This study revealed that  $\text{CoCl}_2 \cdot 2\text{H}_2\text{O}$  has a XANES spectrum with a doublet white line and an absorption edge slightly lower in energy than that of the hexahydrate. This change corresponds to the change in the octahedral coordination sphere of Co(II) from  $6\text{H}_2\text{O}$  in the hexahydrate to  $2\text{H}_2\text{O} + 4\text{Cl}^-$  in the dihydrate [11]. It was also revealed that the peak intensity on the high-energy side of the double white lines decreases when the remaining two  $\text{H}_2\text{O}$  molecules are dissociated and become anhydrous  $\text{CoCl}_2$ . The absorption edge shifts slightly to lower energy when changing from dihydrate to anhydride. The low energy shift appears to be proportional to the number of containing water molecules. A weak pre-peak assigned to the quadrupole transition is observed at 7.708 keV for all of  $\text{Co}(\text{H}_2\text{O})_6\text{Cl}_2$ ,  $\text{CoCl}_2 \cdot 2\text{H}_2\text{O}$ , and  $\text{CoCl}_2$ . In this study, we have succeeded in measuring the XANES spectra of Co(II) chloride with a specific number of hydration waters with high accuracy.

The results of *in-situ* XAFS analysis for the TPR process of  $\text{Co}_3\text{O}_4$  supported on silica have been previously reported [4]. The reduction of  $\text{Co}_3\text{O}_4$  to Co(0) proceeds via a CoO intermediate state. The reduction of  $\text{Co}_3\text{O}_4$  to CoO (eq. (2)) proceeds at around 400 °C, followed by the reduction to Co(0) (eq. (3)) at around 540 °C.



It was revealed that the reduction reaction of  $\text{CoCl}_2$  by  $\text{H}_2$  gas (*ca.* 360 °C) investigated in this study proceeds at a temperature approximately 200 °C lower than that of CoO with the same Co(II) center. The Co(II) center is surrounded by six anions in both cases as shown in Fig. 4. While CoO has a rock-salt structure [12],  $\text{CoCl}_2$  has a layered structure in which

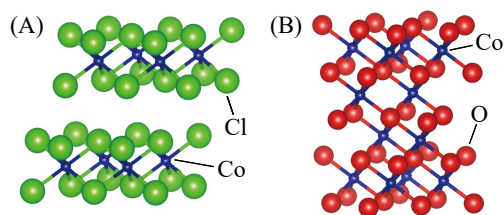


**Fig. 4.** Crystal structure of  $\text{CoCl}_2$  (A) and  $\text{CoO}$  (B).

$\text{CoCl}_6$  octahedrons are arranged in a plane with shared edges [13]. A large difference in the reducibility between  $\text{CoCl}_2$  and  $\text{CoO}$  may be due to the difference in the crystal structure. The layered structure of  $\text{CoCl}_2$  is interpreted as more favorable for the chloride ion dissociation reaction accompanied by the reduction of the  $\text{Co(II)}$  center.

The results of *in situ* XAFS analysis for the reduction process of  $\text{CuCl}_2$  and  $\text{NiCl}_2$  supported on silica by  $\text{H}_2$  have been previously reported [14].  $\text{CuCl}_2$  is first reduced to  $\text{CuCl}$  at  $300\text{ }^\circ\text{C}$ , and the reduction of  $\text{CuCl}$  to  $\text{Cu(0)}$  proceeds at  $390\text{ }^\circ\text{C}$ . The reduction temperature of  $\text{NiCl}_2$  to  $\text{Ni(0)}$  is  $380\text{ }^\circ\text{C}$ .  $\text{NiCl}_2$  [15] and  $\text{CoCl}_2$  [13] have similar crystal structures and their reduction temperatures are also comparable. The standard redox potential for the  $\text{Co}^{2+}/\text{Co}$  pair in aqueous solution is  $-0.277\text{ V}$  vs normal hydrogen electrode (NHE), which is slightly more negative than the corresponding value of  $-0.257\text{ V}$  vs NHE for the  $\text{Ni}^{2+}/\text{Ni}$  pair. The reduction temperature on silica was slightly lower for  $\text{CoCl}_2$ , which was opposite to the tendency of reducibility expected from the standard redox potentials of the metal(II) ion in water.

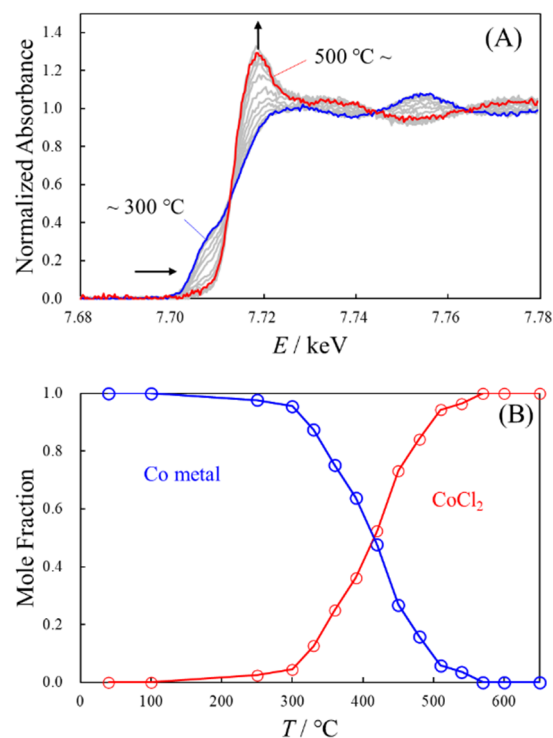
### 3.3. Chlorination Process

Figure 5(A) shows the XANES spectral change during the TPC process of  $\text{Co(0)}$  on silica by gaseous  $\text{Cl}_2$ . The energy resolution in this measurement is inferior to that in the TPR process shown in Fig. 2(A). However, it is clear that the initial state is  $\text{Co(0)}$  and the final state is anhydrous  $\text{CoCl}_2$  with a single white line observed at  $7.72\text{ keV}$ . Because there are some isosbestic points in the spectral change, the chlorination process from  $\text{Co(0)}$  to  $\text{CoCl}_2$  expressed by eq. (4) progresses in one step.



The LCF analysis was performed using the first and last spectra of the TPC process as standards. The temperature change of the obtained composition is given in Fig. 5(B). The state of  $\text{Co(0)}$  was maintained up to  $300\text{ }^\circ\text{C}$ , and the chlorination reaction progressed at around  $420\text{ }^\circ\text{C}$ . It was then converted to  $\text{CoCl}_2$  at temperatures above  $500\text{ }^\circ\text{C}$ .

The results of *in situ* XAFS analysis of the



**Fig. 5.** The change of the XANES spectra (A) and the mole fraction of the Co species (B) during the TPC process of metallic Co on silica.

temperature-programmed oxidation (TPO) process of  $\text{Co(0)}$  supported on silica have been reported [4]. Two oxidation processes,  $\text{Co(0)}$  to  $\text{CoO}$  (eq. (5)) and  $\text{CoO}$  to  $\text{Co}_3\text{O}_4$  (eq. (6)), proceed in parallel in the temperature range of  $100$  to  $300\text{ }^\circ\text{C}$ , and the disappearance of  $\text{Co(0)}$  is completed at about  $300\text{ }^\circ\text{C}$ , which is about  $200\text{ }^\circ\text{C}$  lower than the TPC process (see Fig. 4(B)).



The fact that the formation of  $\text{CoO}$  is completed at a lower temperature than that of  $\text{CoCl}_2$  indicates the relative stability of  $\text{CoO}$  to  $\text{CoCl}_2$  and corresponds to the fact that the reduction of  $\text{CoO}$  requires a higher temperature than that of  $\text{CoCl}_2$  mentioned above.

It has been reported that the surface of the  $\text{Co(0)}$  particles is oxidized when the particles are exposed to  $\text{O}_2$  gas at room temperature [4]. This has also been pointed out for the  $\text{Ni(0)}$  particle on silica [2,3]. In this study, the  $\text{Co(0)}$  particles supported on silica were exposed to  $\text{Cl}_2$  gas. As is clear from Fig. 5, no change was observed in the XANES spectrum at room temperature, indicating that the  $\text{Co(0)}$  state was maintained when exposed to  $\text{Cl}_2$  gas. It is considered that the structural stability of  $\text{CoO}$  allowed the surface oxidation of  $\text{Co(0)}$  particles.

#### 4. Conclusions

In this study, the thermochemical conversion processes between  $\text{CoCl}_2$  and  $\text{Co}(0)$  supported on silica by gaseous  $\text{H}_2$  or  $\text{Cl}_2$  were analyzed by means of *in situ* XAFS method. It has been clarified that the temperature of reduction is lower for  $\text{CoCl}_2$  than for  $\text{CoO}$ , *i.e.*, the dissociation of  $\text{Cl}^-$  from the  $\text{CoCl}_2$  particle occurs more readily than that of  $\text{O}^{2-}$  from the  $\text{CoO}$  particle. This difference was discussed from the perspective of the crystal structure of  $\text{CoCl}_2$  and  $\text{CoO}$ . The chlorination process of  $\text{Co}(0)$  particles by  $\text{Cl}_2$  has been analyzed and it is found that the chlorination reaction requires a significantly higher temperature than the oxidation reaction by  $\text{O}_2$ . These results suggest that there are differences in reactivity in conversion depending on the type of anion.

In this study, samples were prepared by the impregnation method using an aqueous solution of  $\text{CoCl}_2$ , and this technique is widely used in the preparation of catalyst materials. Initially,  $\text{Co}(\text{H}_2\text{O})_6\text{Cl}_2$  was supported on silica while maintaining its hydrated state in aqueous solution. By placing it in a dry environment, it changed to a dihydrate  $\text{CoCl}_2 \cdot 2\text{H}_2\text{O}$  at room temperature, and reached anhydrous  $\text{CoCl}_2$  when heated to about 200 °C. *In situ* XAFS analysis of this process revealed that as the number of  $\text{Cl}^-$  coordinated to  $\text{Co}(\text{II})$  increases from 0 (hexahydrate) to 4 (dihydrate) to 6 (anhydride), the absorption edge energy shifts to the lower side and the shape of the white line changes.

#### Acknowledgement

The XAFS measurements at the Photon Factory (KEK) were performed under the approval of the Photon Factory Program Advisory Committee (Proposal No. 2023G561).

#### References

- [1] S. Yamashita, Y. Yamamoto, H. Kawabata, Y. Niwa, M. Katayama, and Y. Inada, *Catal. Today*, **2018**, *303*, 33.
- [2] Y. Yamamoto, A. Suzuki, N. Tsutsumi, M. Katagiri, S. Yamashita, Y. Niwa, M. Katayama, and Y. Inada, *J. Solid State Chem.*, **2018**, *258*, 264.
- [3] S. Yamashita, Y. Yamamoto, M. Katayama, and Y. Inada, *Bull. Chem. Soc. Jpn.*, **2015**, *88*, 1629.
- [4] S. Chotiwan, H. Tomiga, M. Katagiri, Y. Yamamoto, S. Yamashita, M. Katayama, and Y. Inada, *J. Solid State Chem.*, **2016**, *241*, 212.
- [5] J. Cabana, L. Monconduit, D. Larcher, and M. R. Palacin, *Adv. Mater.*, **2010**, *22*, E170.
- [6] F. Wu and G. Yushin, *Energy Environ. Sci.*, **2017**, *10*, 435.
- [7] A. E. Kharbachi, O. Zavorotynska, M. Latroche, F. Cuevas, V. Yartys, and M. Fichtner, *J. Alloys Compd.*, **2020**, *817*, 153261.
- [8] X. Zhao, S. Ren, M. Bruns, and M. Fichtner, *J. Power Sources*, **2014**, *245*, 706.
- [9] F. Gschwind, H. Euchner, and G. Rodriguez-Garcia, *Eur. J. Inorg. Chem.*, **2017**, *2017*, 2784.
- [10] S. Chen, L. Wu, Y. Liu, P. Zhou, Q. An, and L. Mai, *J. Energy Chem.*, **2024**, *88*, 154.
- [11] B. Morosin, *J. Chem. Phys.*, **1966**, *44*, 252.
- [12] W. Jauch, M. Reehuis, H. J. Bleif, F. Kubanek, and P. Pattison, *Phys. Rev. B*, **2001**, *64*, 052102.
- [13] M. K. Wilkinson, J. W. Cable, E. O. Wollan, and W. C. Koehler, *Phys. Rev.*, **1959**, *113*, 497.
- [14] M. Katayama, Y. Sugimura, S. Nakamura, T. Nishikawa, T. Ishida, and Y. Inada, *Memo. SR Center Ritsumeikan Univ.*, **2023**, *25*, 3.
- [15] A. Ferrari, A. Braibanti, and G. Bigliardi, *Acta Crystallogr.*, **1963**, *16*, 846.